CAMILA Hall Thruster: New Results

IEPC-2011-046

Presented at the 32nd International Electric Propulsion Conference,
Wiesbaden • Germany
September 11 – 15, 2011

A. Kapulkin[1], V. Balabanov[2], M. Rubanovich[3], E. Behar[4]
Asher Space Research Institute – Technion, I. I. T., Haifa, 32000, Israel

L. Rabinovich[5] and A. Warshavsky[6]
Rafael, Haifa, 31021, Israel

Abstract: The paper is devoted to a continuation of experimental investigations of a CAMILA Hall thruster (HT) and optimization of its parameters. The CAMILA HT is a new low-power Hall thruster concept. In the paper, two versions of the CAMILA HT are discussed: a full CAMILA HT where a longitudinal magnetic field in an anode cavity is created by special anode coils and for the first time simplified CAMILA HT, in which in order to create a longitudinal component of the magnetic field in the cavity no additional magnetic coils are applied. Some features of physical processes in simplified CAMILA HT are considered. The magnetic system of simplified CAMILA HT is simpler and it consumes less power, but the anode efficiency of the full CAMILA HT is generally higher. However, an optimization of the magnetic field configuration, in order to make it closer to that in the full CAMILA HT without application of additional coils, carried out recently, allowed essentially increasing the efficiency. The following performance was attained: at discharge power of 198 W, the anode efficiency and specific impulse were 49.6 % and 1622 s, respectively. The expected life time is large than 4000 h. In the paper, the preliminary results of discharge current oscillations are presented. Increasing the longitudinal magnetic field in the anode cavity reduced amplitude of oscillations.

Nomenclature

B	=	magnetic field induction
D_{in}	=	inner diameter of anode cavity
D_{ou}	=	outer diameter of anode cavity
E	=	electrical field strength
e	=	unit charge
F	=	thrust
h	=	width of anode cavity
I_{asp}	=	anode specific impulse
j_{ec}	=	density of electron current, collected by electrode
l_p	=	depth of plasma penetration into anode cavity
m	=	mass of electron
n	=	density of electrons
n_a	=	density of atoms
P	=	discharge power
Q_{ea}	=	cross-section of electron-atom collisions
S	=	cross-section of anode cavity
T_e	=	temperature of electrons

[1] Leading Researcher, Head of Electric Propulsion Lab, kapulkin@tx.technion.ac.il.
[2] Leading Researcher, Head of Mechanic Group, balaban@tx.technion.ac.il.
[3] Engineer, Electric Propulsion Lab, aerrumax@tx.technion.ac.il.
[4] Director of Institute, Professor of Physical Department of Technion, behar@physics.technion.ac.il.
[5] Project Manager, leonidr@rafael.co.il.
[6] System Engineer of Electric Propulsion, avrahamw@rafael.co.il.

U_a = near anode fall of potential
U_d = discharge voltage
U_{max} = fall of potential between its maximum inside cavity and exit of cavity
v_e = velocity of electron
v_{eth} = thermal velocity of electrons
η_a = anode efficiency
ω_e = electron cyclotron frequency
θ = average angle between magnetic field line and radius of anode cavity
τ_{ea} = time of electron free moving due to electron-atom collisions

I. Introduction

AT present, much attention is being given to a development of low power Hall thrusters (50 – 300 W) for applications on micro-spacecraft[1-12]. At building such thrusters, the high efficiency often conflicts with an acceptable lifetime due to the difficulty of attaining the high mass efficiency in small power thrusters[13]. In order to solve the problem, a new concept of low power Hall thrusters has been proposed[14] and named the CAMILA (Co-Axial Magneto-Isolated Anode) Hall thruster. The initial experiments, carried out with the 200 W-class model at Soreq NRC[15] confirmed the expected high efficiency and demonstrated an anode efficiency exceeding 43% at a power of 200 W. The expected lifetime of this model was at least 4000 h, owing to relatively low ion-current density (the outer diameter of the acceleration channel and its width were 55 mm and 12 mm, respectively) and rather thick walls. In Ref. 16, a theoretical evaluation was performed for determining the appropriate longitudinal magnetic field, which should provide the desired configuration of the electric field and its magnitude in the anode cavity of the CAMILA Hall thruster.

The present paper is devoted to further investigations of processes in the CAMILA Hall thruster and optimization of its operation parameters.

II. Two Versions of CAMILA Hall Thruster

A schematic of the CAMILA Hall thruster with simulated magnetic field is shown in Fig.1. The ionization of propellant is produced mainly in the anode cavity that is formed by two co-axial metallic cylinders, which are kept under the anode potential, and an end face of the gas-distributor which is under a floating potential. In the anode cavity, the longitudinal magnetic field is applied. It is produced by outer and inner anode magnetic coils with electric currents in opposite directions and the magnetic screens. The propellant, entering the cavity through the gas distributor, is ionized by electrons, which oscillate between the end face of the gas-distributor and the exit of the cavity. At a sufficiently strong magnetic field in the cavity, it is possible to form a radial electric field, directed to the middle surface of the cavity, in spite of the radial gradient of electron pressure. This radial electric field keeps ions from colliding with the cylindrical walls of the cavity. (The length of the cavity can be varied to obtain a high degree of propellant ionization.) After leaving the anode cavity, the ions are accelerated by a longitudinal electric field in the acceleration channel.

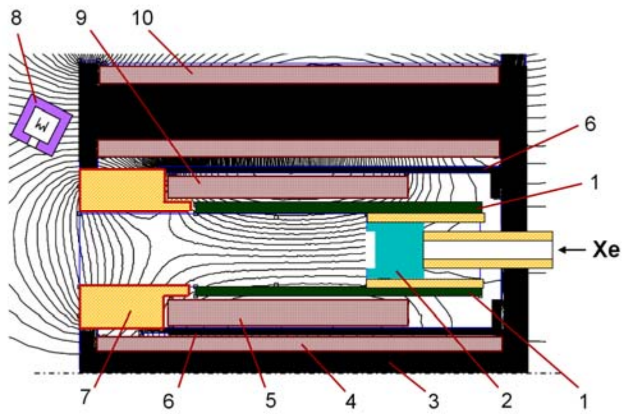

1 – Anode, 2 – Gas-distributor, 3 – Magnetic circuit, 4 – Central magnetic coil, 5 – Inner anode coil, 6 – Magnetic screens, 7 – Acceleration channel wall, 8 – Cathode-neutralizer, 9 – Outer anode coil, 10 – Outer magnetic coils.

Figure1. Schematic of CAMILA Hall thruster

The experimental investigations showed that rather high anode efficiency can be obtained, even in the simplified version of the CAMILA Hall thruster (Fig. 2), where a longitudinal component of the magnetic field in the anode cavity is created with only basic magnetic coils (outer and central), that is, without using the anode coils. In this case, a magnetic system is lesser complex and consumes less power.

III. Some features of physical processes in simplified CAMILA Hall thruster

A. General remarks about processes in anode cavity

First of all, it is necessary to note that the fact that all magnetic field lines in the anode cavity of the simplified CAMILA Hall thruster intersect an anode surface means that at rather high temperature of electrons a plasma potential should exceed the potential of the anode in a significant part of the anode cavity. This follows from the necessity to reconcile the magnitude of a thermal flux of the electrons from the plasma to the anode surface with the magnitude of a discharge current. This, in turn, means that heating the electrons in the cavity can not be self-sustained. In order for, the electrons can ionize atoms in the cavity, they should come from the acceleration channel or get energy from the electrons which come from the acceleration channel. These can be the electrons, which go from the cathode and also the electrons which were born in the process of ionization of atoms in the acceleration channel and were heated by an electrical field in the ionization area.

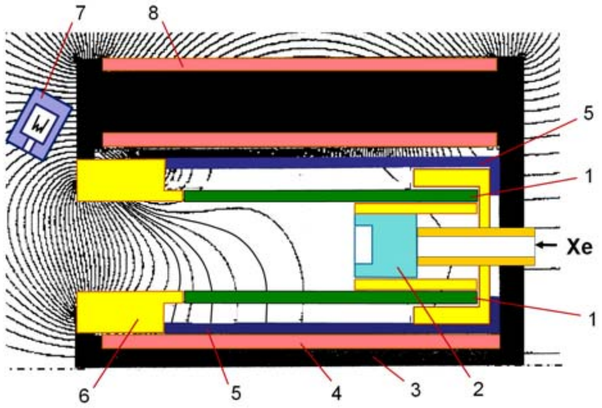

1 – Anode, 2 – Gas-distributor, 3 – Magnetic circuit, 4 – Central magnetic coil, 5 – Magnetic screens, 6 – Acceleration channel wall, 7 – Cathode-neutralizer, 8 – Outer magnetic coils.

Figure 2. Schematic of simplified CAMILA Hall thruster

B. Estimation of depth of plasma penetration into anode cavity

In order for, the electrons from the acceleration channel can ionize atoms, they should penetrate to the cavity crossing the magnetic field. In spite of the fact that magnetic field lines in the cavity intersect the outer dielectric wall of the acceleration channel, the near wall conductivity, probably, do not play essential role in the transfer of the electrons across the magnetic field. This is due to the strong magnetic mirror effect near the outer wall. Only the very small fraction of the electrons can reach the wall. For this reason, the electrons in the cavity should not be cooled by the wall.

We will make a rough estimation of a depth of the plasma penetration into the anode cavity. Here, the term depth of plasma penetration is used to mean a distance from cavity exit to a place inside the cavity where potential attains a maximum. For simplicity, we will neglect of a magnetic field line slope with respect to the radius of the anode cavity.

The density of an electron current collected by an electrode, if it is less than a density of chaotic current, is defined, as well known, by the formula:

$$j_{ec} = \frac{env_{eth}}{4} e^{-\frac{eU_a}{T_e}} \tag{1}$$

Where e – the unit charge,

n – the density of electrons,

$v_{eth} = \sqrt{\frac{8T_e}{\pi m}}$ - the thermal velocity of electrons,

T_e – the temperature of electrons,

m – the mass of electron

U_a – the near anode fall of potential.

On the other hand, the electrons can move along the cavity under the influence of a longitudinal electric field. The density of the electron current along the cavity is

$$j_{el} = \frac{ne^2}{m\omega_e^2 \tau_{ea}} E \tag{2}$$

Where E – the strength of electrical field,

$\omega_e = \frac{eB}{m}$ - the electron cyclotron frequency,

B - the magnetic field induction,

$\tau_{ea} = \frac{1}{n_a < Q_{ea} v_e >}$ – the time of electron free moving due to electron-atoms collisions,

n_a – the density of atoms,

Q_{ea} – the cross-section of electron-atom collision,

v_e - the electron velocity.

Equating the approximate expression for the current which the inner anode collects to the approximate expression for the current which passes along the anode cavity (with taking into account Eqs.(1,2), we obtain:

$$\frac{env_{th}}{4}e^{-\frac{eU_a}{T_e}}D_{in}l_p=\frac{ne^2ES}{m\omega_e^2\tau_{ea}} \tag{3}$$

Where D_{in} – the diameter of the inner anode,

l_p – the depth of the plasma penetration,

$S=0.5\cdot\pi(D_{ou.}+D_{in})\cdot h$ – the cross-section of the anode cavity,

D_{ou} – the diameter of outer anode,

h – the width of the anode cavity.

We assume that 1) the electrical field strength and near anode fall of the potential are constants and equal, respectively:

$$E=\frac{U_{\max}}{l_p}\ ,\quad U_a=\frac{U_{\max}}{2}\ ,$$

Where U_{max} - the difference potentials between exit of the anode cavity and its maximum inside the cavity.
Substituting expressions for E and U_a in Eq.(4), we obtain the following rough estimation for the depth of plasma penetration into the anode cavity:

$$l_p=\frac{2e^{\frac{eU_{\max}}{4T_e}}}{\omega_e}\left(\frac{eU_{\max}S}{m\tau_{ea}V_{eth}D_{in}}\right)^{1/2} \tag{4}$$

We will make a numerical evaluation of l_p for typical parameters of the anode cavity. We assume that $U_{max}\approx T_e/e = 10$ V. At $D_{in} = 3.1\cdot10^{-2}$ m, $D_{ou} = 5{,}5\cdot10^{-2}$ m, $h = 1.2\cdot10^{-2}$ m, mass flow rate of Xenon equal to $0.776\cdot10^{-6}$ kg/s, and velocity of Xenon flux in the cavity equal to 200 m/s, we have $n_a = 1.11\cdot10^{19}$ m^{-3}. Then at $T_e = 10$ eV, we obtain $\tau_{ea} = 7.63\cdot10^{-8}$ s and $V_{eth} = 2.11\cdot10^{6}$ m/s. In this case, at $B = 2.5\cdot10^{-3}$ T, we have from Eq.(4) $l_p = 4.4\cdot10^{-3}$ m. Taking into account magnetic field line inclinations with respect to the radius of the anode cavity increases the depth of the plasma penetration by a factor of 1.5 – 2.

C. Influence of magnetic field non-uniformity on processes in anode cavity

Because of an inverse dependence of electron mobility on the square of the transverse magnetic field induction, electrons should intersect the magnetic field mainly in the place, where it has a minimum, i.e. mainly a short distance from the inner anode surface. The most of the penetrated electrons and electrons born as a result of ionized process cannot move along the magnetic field lines to a significant distance from the inner anode surface because of the strong magnetic mirror effect. These two factors must bring about some radial non-uniformity of the plasma density in the anode cavity. This physical model is consistent with results of numerical modeling the processes in the simplified CAMILA Hall thruster by PIC method, where such radial non-uniformity of plasma in the anode cavity was found[17].

On the other hand, a retardation of the electrons by the magnetic mirror effect near a middle surface of the cavity together with the magnetic isolation of the outer anode must reduce the plasma potential in this area in comparison with the potential in the vicinity of the anodes. This, in turn, must form the focusing structure of equipotential surfaces as in the area of plasma penetration (in the sense, defined in previous section!), so at the entrance to the acceleration channel. Thus, the conditions for preventing a disappear of the ions on walls of the ionization area are created.

IV. Experimental Investigations of Simplified CAMILA Hall Thruster

The experimental investigations were carried out in new Electrical Propulsion Laboratory of the Asher Space Research Institute at the Technion, which includes a vacuum chamber of 3.2 m^3. A cryogenic pumping system provided the residual gas pressure not exceeding $6\cdot10^{-8}$ mBar and the Xenon pressure not exceeding $2\cdot10^{-5}$ mBar at a total mass flow rate of 1mg/s.

The experiments were mostly performed with CAMILA HT-55 model (Fig.3), having the acceleration channel outer diameter of 20 mm and the width of the channel of 55 mm. This is 200 W-class model. It is described in detail in Ref. 10. The model allows for many different experimental set ups. Some experiments were carried out with the model CAHT-55, having the same sizes that CAMILA HT-55, but the design of which meets the requirements to a flying model. It is shown in Fig.4.

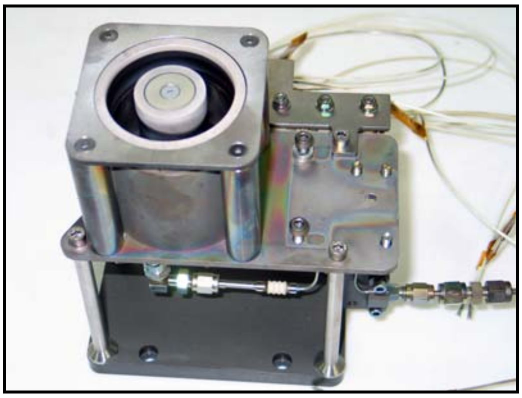

Figure 3. Experimental model of CAMILA Hall thruster (CAMILA-HT-55)

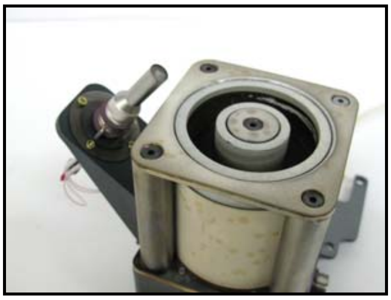

Figure 4. Model of CAMILA Hall thruster CAHT-55

The experiments were carried out with two length of the anode cavity. The shorter anode had the length by 30 % less than long one.

In the course of the experimental investigations, mass flow rates ranged from 0.65 to 1.5 mg/s. The discharge voltage was varied from 250 to 300 V. The mass flow rate through the cathode-neutralizer was 0.25 mg/s in almost all experiments. The industrial cathode could not operate in self-sustained mode at a discharge current of less than 1 A. Therefore in the experiments, additional heating of the cathode emitter was performed by the use of an auxiliary discharge between it and a cathode keeper. The voltage between the keeper and emitter was kept at levels of 14 - 20 V.

A. Performance of thruster

In Fig. (5 – 7), Fig. (8 – 10), and Fig. (11 – 13), the dependences of the thrust, anode specific impulse, and anode efficiency for two length of the anode cavity on the discharge power at the discharge voltages of 250 V, 275 V and 300 V respectively, are presented. First of all, it is necessary to note that over the investigated region of powers from 140 W to 400 W, at all investigated voltages, the anode efficiency of the simplified CAMILA Hall thruster exceeds 40 %. The exception is only the small area within 160 W at operation with long anode and voltage of 250 V. To this, one should be added the following. Though, the experiments carried out mainly with the use of the industrial cathode, which could not run in self-sustained mode, nevertheless in some experiments was applied a cathode-neutralizer, developed at KhAI (Ukraine) in group of A. Loyan. (This cathode operated in the self-sustained mode with a Xe-consumption of 0.15 mg/s.) The results were close to those, which obtained at the experiments with the industrial cathode. For example, at operation of the CAHT-55 model with KhAI's cathode the anode efficiency of 42.5 % and anode specific impulse of 1528 s were attained at the power of 180 W and discharge voltage of 300 V.

From the data, presented in the Fig.7,10,13 it follows that the preferential length of the anode depends on the discharge voltage. At voltage of 250 V, the higher efficiency was attained for the shorter anode. At 275 V and 300 V over all investigated powers, the efficiency is higher at the long anode. The possible reason is, probably, a competition between the growth of ability to ionize atoms with increasing the length of the anode cavity and difficulty of extracting the ions from the long cavity. The latter is earthier realized at the larger discharge voltages.

B. Distribution of discharge current between inner and outer anodes

The design of the experimental model CAMILA HT-55 allows separately measuring discharge current fractions entering the inner and outer anodes. The carried out experiments showed that there is a strong asymmetry in a distribution of the discharge current between inner and outer anodes. The current to the inner anode exceeded always the current to the outer anode in spite of the fact that an area of inner anode is less than an area of the outer one. In some experiments the excess was as great as two orders of a magnitude. This can be explained with the magnetic isolation of the outer anode.

V. Results of Experimental Investigations of Full CAMILA Hall Thruster performance

The experiments showed that if the currents were supplied to anode coils in the thruster with long anode, no essential change in the performance of the thruster took place in comparison with the simplified CAMILA Hall thruster. This was due to the fact that at the currents in the anode coils, which did not exceed the acceptable (with the point of view of coil's heating) values, the longitudinal magnetic field induction was significantly less than the radial magnetic field in the acceleration channel. As a result, the magnetic field configuration in the anode cavity noticeably differed from that is shown in Fig.1. The magnetic field lines intersected the surface of the anode. In this situation, the simplest that could be done it was reducing the length of the anode by moving the gas distributer into the anode cavity. In position, which was defined in the previews section as short anode, the most of the magnetic field lines ceased to intersect the surface of the anode. They intersected the surface of the gas-distributor. As a result, the anode efficiency and specific impulse of the thruster increased (Fig.14-19). These exceeded not only the efficiency and specific impulse of the simplified CAMILA Hall thruster with the short anode, but also the efficiency and specific impulse of the thruster with the long anode, including the operation modes with the discharge voltage of 300 V. The exceptions are the areas of the smallest powers (140 – 150 W) as in the case of the short anode, so at the long anode. Probably in these power areas, the configuration and induction of the longitudinal magnetic field should be chosen more carefully. (The data, illustrated in Fig.(14-19), related to the same currents in the anode coils independently on the discharge power and discharge voltage.)

The investigations showed that there exist the optimal values of the currents in the anode coils at which the anode efficiency of the thruster attains a maximum.

VI. Optimization of Magnetic Field Configuration in Simplified CAMILA Hall Thruster

Most recently, the optimization of the magnetic field configuration in the simplified version of CAMILA Hall thruster was carried out. As a result, in the anode cavity, an average ratio of the magnetic field longitudinal component to the radial component was increased from 1.1 to 2.3 without application of the anode magnetic coils. This gave rise to an additional improvement of the thruster performance, especially in the range of 150 – 250 W. Some results of the experimental investigations of the simplified CAMILA Hall thruster with optimized magnetic field are presented in a table.

Table

P, W	U_d, V	$\dot{m}$, mg/s	F, mN	η_a, %	I_{spa}, s
153.8	250	0.700	9.65	43.2	1405
165.0	275	0.680	10.40	48.1	1558
198.0	275	0.776	12.35	49.6	1622
252.4	275	0.970	16.05	52.5	1686
295.2	300	0.970	17.80	55.3	1870

The optimization of the magnetic field configuration brought about a redistribution of the discharge current between anodes. The current, which collected with the inner anode, reduced by a factor of ~ 1.5. This can be explained by decreasing an angle of the entry of the electrons into the inner anode, due to growth of the longitudinal component of the magnetic field.

VII. Experimental Investigations of Discharge Current Oscillations

The experimental research of low-frequency oscillations of the discharge current in the CAMILA Hall thruster showed that these resemble those of the conventional Hall thruster. The spectrum of oscillations was essentially dominated by a mode with a frequency of around 20 kHz. The amplitude of this mode was the highest when the currents in the anode magnetic coils were absent, that is, in the simplified version of the CAMILA Hall thruster. The amplitude progressively decreased as the values of the current in the anode magnetic coils increased. In Figure 20, the dependence of the discharge current oscillation amplitude on the discharge power is presented for zero value of anode coil current and for an anode coil current of 2.65 A. The discharge voltage is 250 V in both cases. The possible reason of such influence of the currents in the anode coils is extending the area of the anode surface, accessible for the discharge current.

Conclusion

The carried out investigations showed that:

1. Along with full CAMILA Hall thruster, its simplified version also possesses high anode performance in the field of small powers. The simplification relates to a magnetic system, which is lesser complex and consumes less power.
2. In the frame of the approximate estimation, the plasma should penetrate rather deeply into the anode cavity of the simplified CAMILA Hall thruster.
3. The optimal length of the anode cavity of the simplified CAMILA Hall thruster, at which the maximum of the anode efficiency is provided, depends on a discharge voltage. The possible reason is, probably, a competition between the growth of ability to ionize atoms with increasing the length of the anode cavity and difficulty of extraction the ions from the long cavity. The latter is earthier realized at the larger discharge voltages.
4. The distribution of the discharge current between inner and outer anode of the simplified CAMILA Hall thruster is strongly asymmetric. This can be explained with the magnetic isolation of the outer anode.

5. The anode efficiency of the full CAMILA Hall thruster is higher of the simplified version. A maximum of exceeding was observed at the discharge voltage of 300 V and attained 8.5 % (that is, the ratio of two efficiencies was 1.085).
6. The optimization of the magnetic field configuration in the simplified version of the CAMILA Hall thruster allowed essentially improved the performance of the thruster, especially in the region of 150 – 250 W. The following performance was attained: at power of 154 W - the anode efficiency is 43 %, anode specific impulse is 1405 s, at power of 198 W – the anode efficiency is 49,6 %, anode specific impulse is 1622 s.
7. The low-frequency oscillations of the discharge current in the simplified version of CAMILA Hall thruster resemble those of conventional Hall thruster. The application of the anode magnetic coils, which create the additional longitudinal magnetic field, decreased essentially the amplitude of the oscillations. The possible reason of such influence of the currents in the anode coils is extending the area of the anode surface, accessible for the discharge current.

Acknowledgments

The authors are grateful to Gaby Appelbaum for his help in the work. The authors would like also to thank Dr. Yevgeny Raitses and Prof. Michael Keidar for fruitful discussions.

References

[1]Hruby, V., Monheiser, J., Pote, B., Rostler, P, Kolencik, J., and Freeman, C., "Development of Low Power Hall Thrusters," *The 30th Plasmadynamics and Lasers Conference,* Norfolk, VA, 28 June – 1 July, 1999, AIAA 99-3534.

[2]Hruby, Vlad, (Busek Co. Inc), "Review of Electric Propulsion Activities in the US Industry," *The 39th AIAA/ASME/SAE/ASEE Joint Propulsion Conference and Exhibit*, Huntsville, Alabama, 20 -23 July, 2003, AIAA 2003-4441.

[3]Kulagin, S. N., Statsenko, I. N., Protsan, Yu. V., Ozimin, V. O., Dubovik, L. G., Gontarev, Yu. K., "Electric Rocket Engines of Small Power for Micro-Satellites," *Universities' Projects of Microsatellites: Trends, Technologies, Realization*, Suzir'ya, Dniepropetrovsk, Ukraine (in Russian), 2002, pp. 67 – 72.

[4]Bugrova, A. I., Desiatskov, A. D., Kaufman, H. R., Kharchevnikov, V. K., Morozov, A. I., Zhurin, V. V., "An Improved Small Closed Drift Thruster with Both Conducting and Dielectric Channels," *The 28th International Electric Propulsion Conference*, Toulouse, France, March 17 –21, 2003, IEPC-2003-263.

[5]Bugrova, A. I., Lipatov, A. S., Baranov, S. V., Morozov, A. I., and Daren, Yu., "SPT Operation in Mashine-Gun Mode," *The 29th International Electric Propulsion Conference*, Princeton University, NJ, October 31 – November 4, 2005, IEPC-2005-161.

[6]Ashkenazy, J., Shitrit, S., and Appelbaum, G., "Hall Thruster Modification for Reduced Power Operation," *The 29th International Electric Propulsion Conference*, Princeton University, NJ, October 31 – November 4, 2005, IEPC-2005-080.

[7]Antropov, N. N., Kim, V., Kozlov, V. I., Popov, G. A., and Skrylnikov, A. I., "Small Electric Propulsion Developed by RIAME MAI," *Europian Conference for Aerospace Science (EUCASS 2005)*, Moscow, Russia, July 4 – 7, 2005.

[8]Loyan, A. V., Maksymenko, T. A., "Performance Investigation of SPT-20M Low Power Hall Effect Thruster," *The 30th InternationalElectric Propulsion Conference,* Florence, Italy, September 17 – 20, 2007, IEPC-2007-100.

[9]Belikov, Mikhail B., Gorshkov, Oleg A., Dyshlyuk, Evgeny N., Lovtzov, Aleksandr S., and Shagayda , Andrey A., "Development of Low-Power Hall Thruster with Lifetime up to 3000 Hours," *The 30th InternationalElectric Propulsion Conference,* Florence, Italy, September 17 – 20, 2007, IEPC-2007-129.

[10]Raitses, Yevgeny, Smirnov, Artem, Granstedt, Erik, and Fisch, Nathaniel J., "Overrun Discharge Current Operation of Low Power Cylindrical Hall Thrusters," *The 30th International Electric Propulsion Conference,* Florence, Italy, September 17 – 20, 2007, IEPC-2007-222.

[11]Polzin, K. A, Sooby, E. S., Kimberlin, A. C., Raitses, Y., Smirnov A., and Fish, N. J., "Performance of a permanent-magnet cylindrical Hall-effect thruster, *The 45th AIAA/ASME/SAE/ASEE Joint Propulsion Conference,* Denver, Colorado, 2 – 5 August, 2009, AIAA 2009-4812.

[12]Leufroy, A., Gibert, T., and Bouchoule, A., "Characteristics of a permanent magnet low power Hall thruster," *The 31st International Electric Propulsion Conference,* University of Michigan, Ann Arbor, Michigan, USA, September 20 – 24, 2009, IEPC-2009-083.

[13]Ahedo, E., and Gallardo, J. M., "Scaling Down Hall Thrusters," *The 28th International Electric Propulsion Conference*, Toulouse, France, March 17 –21, 2003, IEPC-2003-104.

[14]Kapulkin, A., Guelman, M., Balabanov, V., and Rubin, B., "Low-Power Hall Thruster," EU Application No/Patent No. 07827357.0 – 1226 PCT/IL2007001384, filed 11 Nov. 2007, Priority US/09.11.06/USP 865033.

[15]Guelman, M., Kapulkin, A., Balabanov, V., Rabinovich, L., Appelbaum, G., "A New Low-Power Hall Thruster Concept," *The 59th International Astronautical Congress,* Glasgow, Scotland, 29 Sep – 3 Oct 2008, IAC-08-C4.4.6.

[16]Kapulkin A., Guelman M., "Theoretical modeling of Ionization Processes in Anode Cavity of CAMILA Hall Thruster," *The 31st International Electric Propulsion Conference, University of Michigan,* Ann Arbor, Michigan, USA, Sep 20 – 24, 2009, IEPC-2009-068.

[17]Kronhaus I., Kapulkin A., Guelman M., and Natan B., "Modeling Physical Processes in CAMILA Hall Thruster by PIC Method," *The 32nd International Electric Propulsion Conference,* Wiesbaden, Germany, September 11 -15, 2011, IEPC-2011-043.

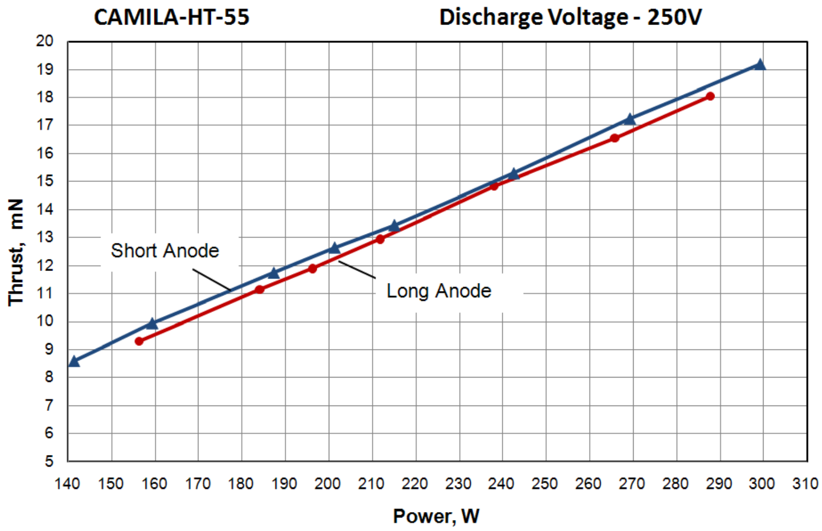

Figure 5. Thrust of simplified CAMILA Hall thruster (U_d = 250V)

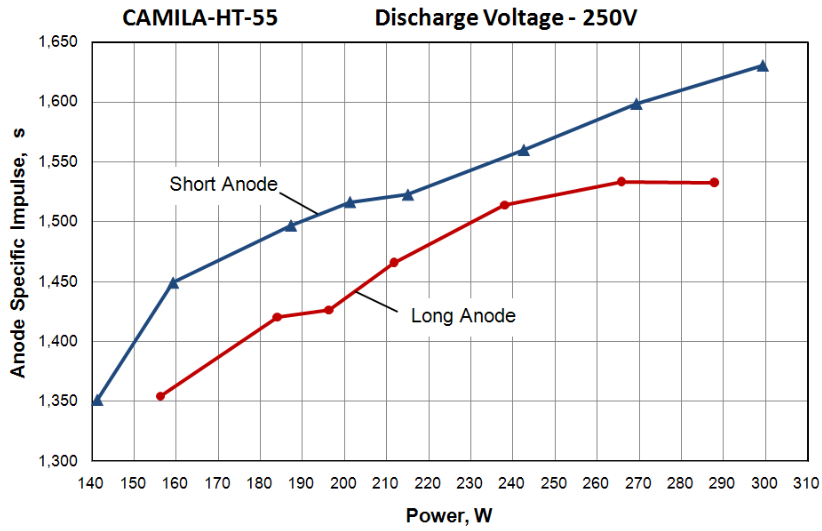

Figure 6. Anode specific impulse of simplified CAMILA Hall thruster (U_d = 250V)

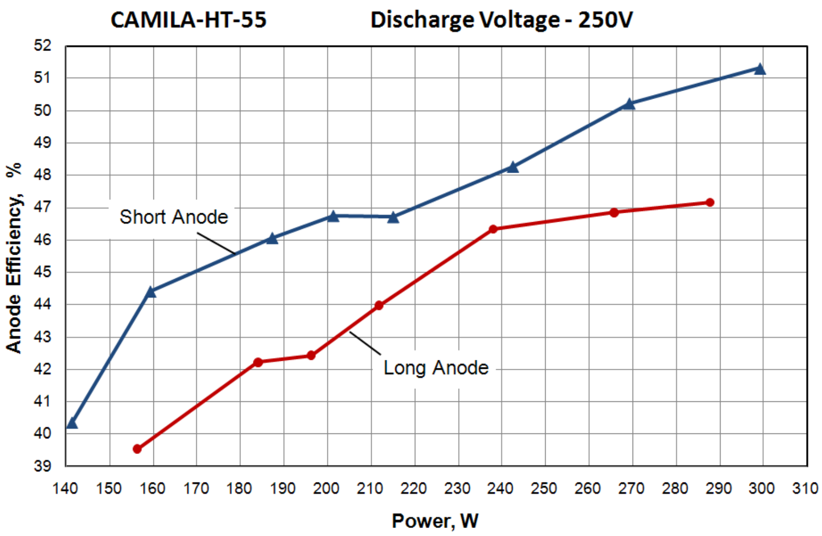

Figure 7. Anode efficiency of simplified CAMILA Hall thruster (U_d = 250V)

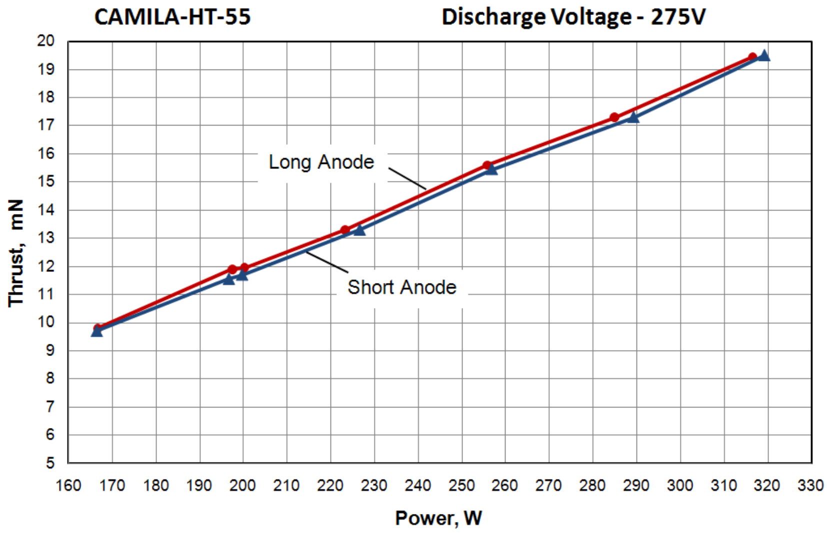

Figure 8. Thrust of simplified CAMILA Hall thruster (U_d = 275V)

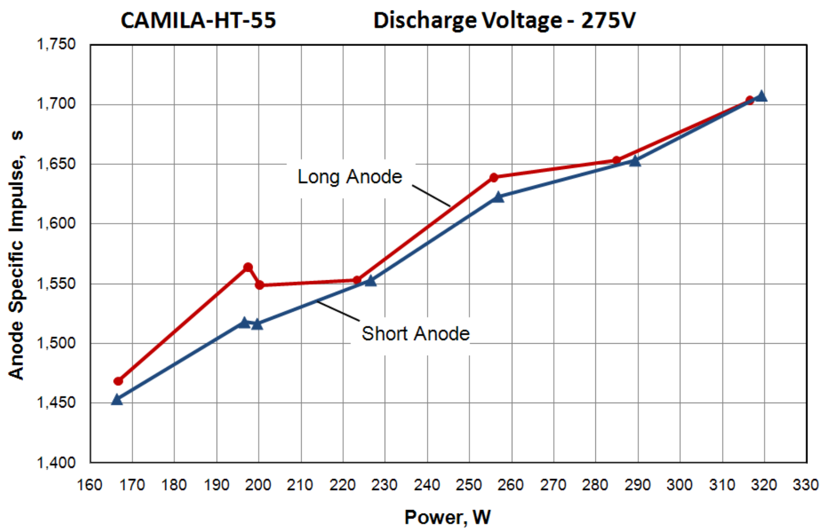

Figure 9. Anode specific impulse of simplified CAMILA Hall thruster (U_d = 275V)

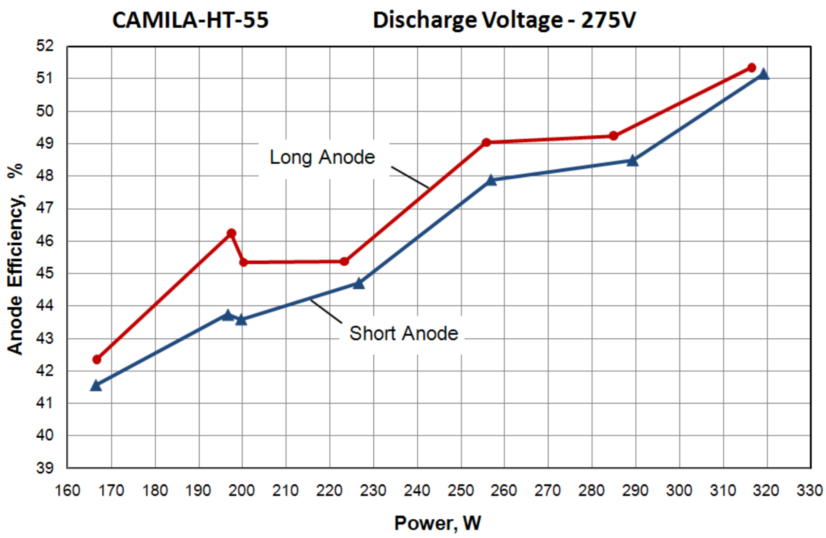

Figure 10. Anode efficiency of simplified CAMILA Hall thruster (U_d = 275V)

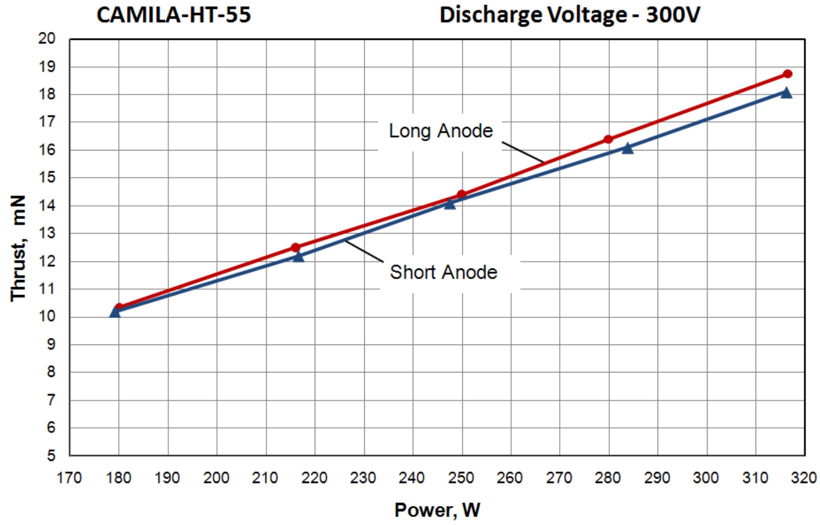

Figure 11. Thrust of simplified CAMILA Hall thruster (U_d = 300V)

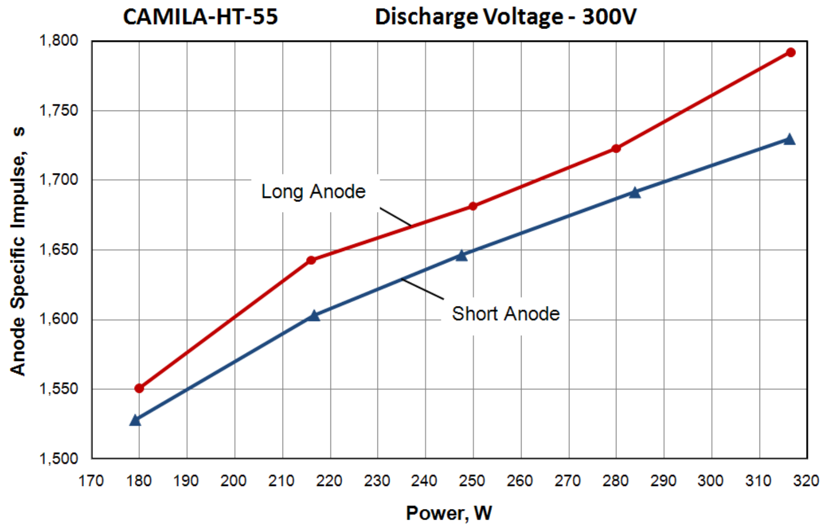

Figure 12. Anode specific impulse of simplified CAMILA Hall thruster (U_d = 300V)

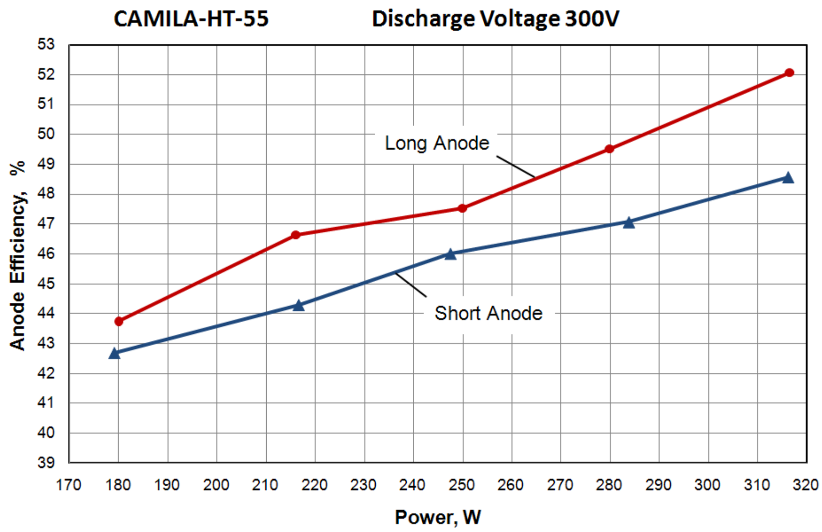

Figure 13. Anode efficiency of simplified CAMILA Hall thruster (U_d = 300V)

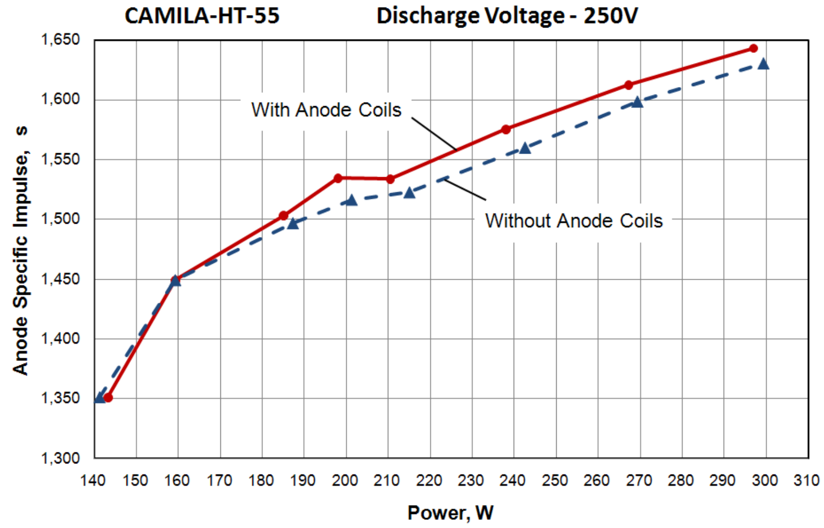

Figure 14. Anode specific impulse of full CAMILA Hall thruster (U_d = 250V)

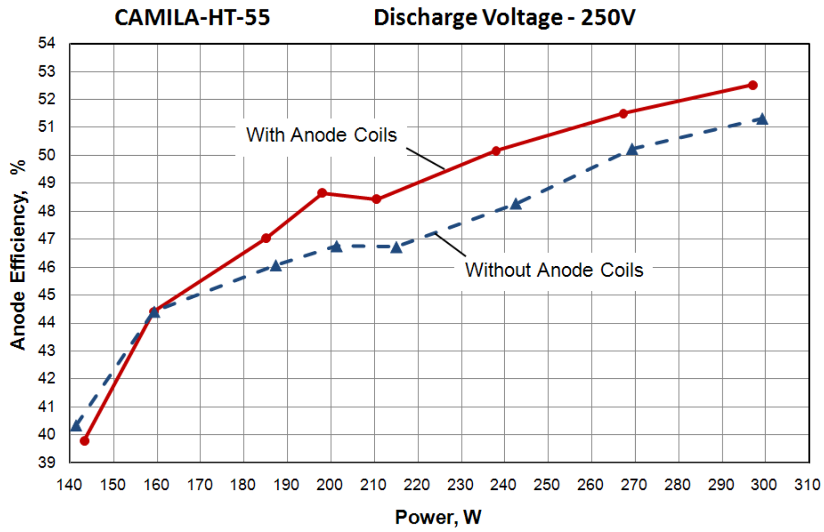

Figure 15. Anode efficiency of full CAMILA Hall thruster (U_d = 250V)

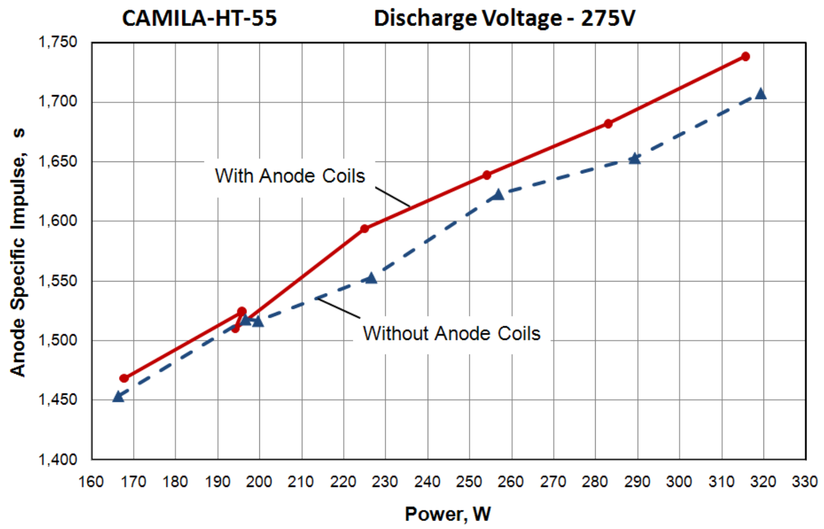

Figure 16. Anode specific impulse of full CAMILA Hall thruster (U_d = 275V)

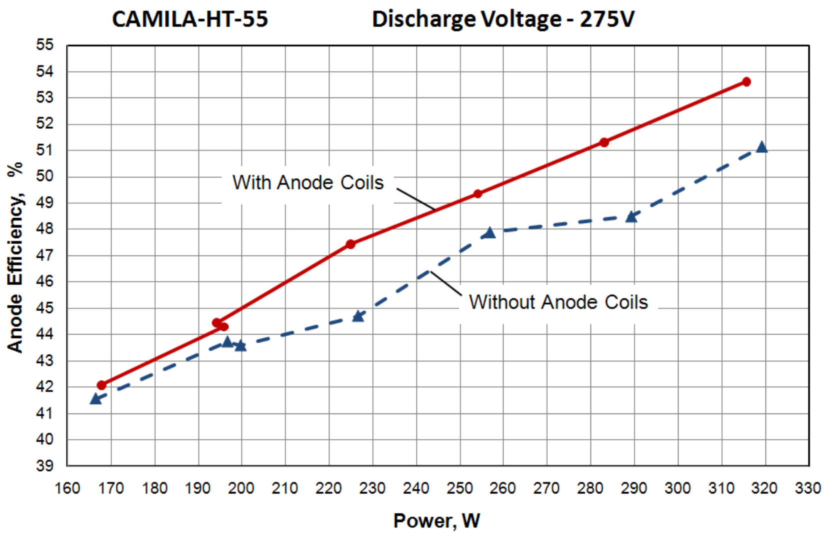

Figure 17. Anode efficiency of full CAMILA Hall thruster (U_d = 275V)

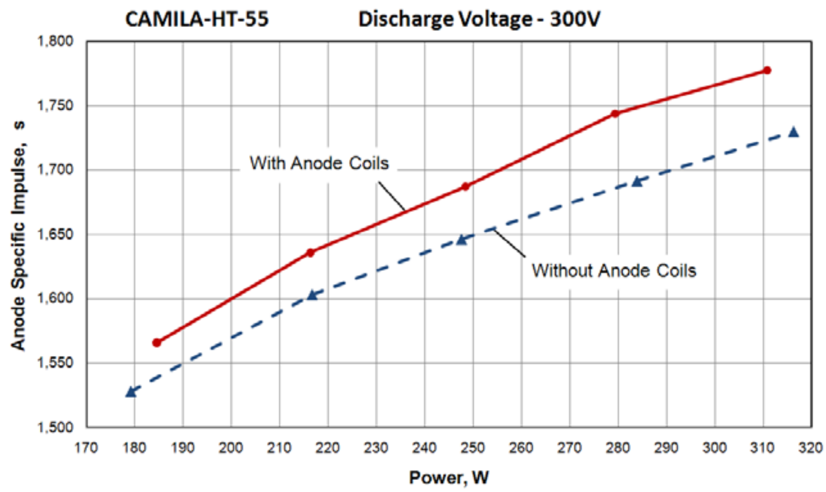

Figure 18. Anode specific impulse of full CAMILA Hall thruster (U_d = 300V)

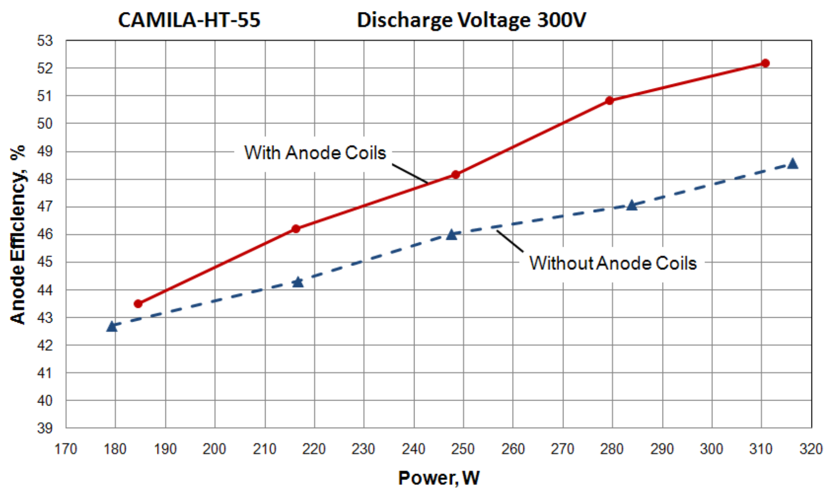

Figure 19. Anode efficiency of full CAMILA Hall thruster (U_d = 300V)

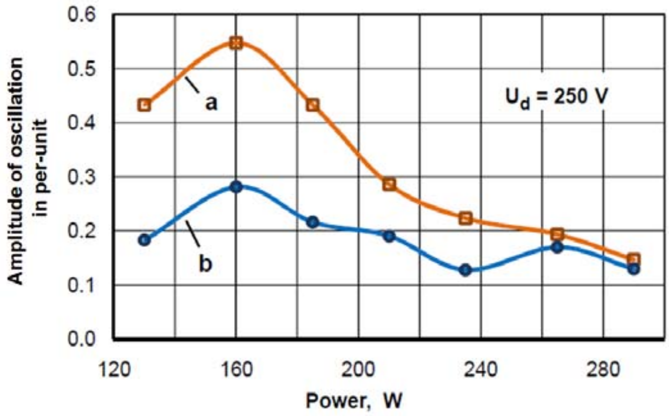

a – without currents in anode coils;
b - with currents in anode coils.

Figure 20. Amplitude of low-frequency oscillation in CAMILA Hall thruster versus power